

Non-Abelian topological insulators from an array of quantum wires

Eran Sagi and Yuval Oreg

Department of Condensed Matter Physics, Weizmann Institute of Science, Rehovot, Israel 76100

(Dated: December 6, 2024)

We suggest a construction of a large class of topological states using an array of quantum wires. First, we show how to construct a Chern insulator using an array of alternating wires that contain electrons and holes, correlated with an alternating magnetic field. This is supported by semi-classical arguments and a full quantum mechanical treatment of an analogous tight-binding model. We then show how electron-electron interactions can stabilize fractional Chern insulators (Abelian and non-Abelian). In particular, we construct a relatively stable non-Abelian \mathbb{Z}_3 parafermion state. Our construction is generalized to alternating wires with spin-orbit couplings, which then gives rise to integer and fractional (Abelian and non-Abelian) topological insulators. The states we construct are effectively two-dimensional, and are therefore less sensitive to disorder than one-dimensional systems. The possibility of experimental realization of our construction is addressed.

PACS numbers: 73.21.Hb, 71.10.Pm, 73.43.-f, 05.30.Pr

Introduction: The integer quantum Hall effect (IQHE) [1] was discovered in two dimensional systems subjected to a strong perpendicular magnetic field. It was quickly understood that disorder and edge modes [2] play an important role in the comprehension of these states. Thouless et al. [3] showed that the quantized conductance is a consequence of the emergence of a topological number, known as the Chern number.

Haldane [4] showed that a Graphene-like material which breaks time reversal symmetry due to an alternating (zero average) magnetic field may have a non-zero Chern number as well. These types of materials, which have a non-zero Hall conductance with a zero total magnetic flux, are referred to as Chern insulators (CI).

The existence of edge modes in the QHE can be understood in various ways. In particular, one can understand the presence of edge modes by studying the classical curved trajectories of electrons in a magnetic field. In fact, it is possible to construct a semi-classical theory for a specific set of Chern insulators as well. The key point is to notice that while at the bottom of the band the effective mass of the electrons is positive, at the top (when the particles are considered as holes) it is negative. Hence, in the presence of an external magnetic field, the trajectories of electrons and holes will be curved in opposite directions.

Let us imagine now a system that consists of a checkerboard of separate regions, containing only electrons or holes. If the electron regions have a positive magnetic field and the hole regions have a negative field, then the trajectories will curve in both regions in the same direction. In the bulk of the system we will have periodic trajectories (that may encircle several checkerboard squares) and near the edge we will have skipping orbits, like the case of electrons in a constant magnetic field.

We note that in principle the particle's motion in the checkerboard construction can be quantized using the Bohr-Sommerfeld quantization condition, leading to ef-

fective Landau levels. However, since the transition between different regions is affected by the specific details of the model, we expect that the resulting bands should not be flat in general.

Motivated by this semi-classical picture, we will study in this work an effectively two-dimensional system which consists of alternating wires that contain electrons and holes. Approaching the 2-dimensional problem from the quasi-one-dimensional (Q1D) limit will allow us to perform a full quantum-mechanical analysis, and treat interaction effects analytically using the one-dimensional bosonization technique for the wires.

Ref. [5] argues that it is possible to understand the IQHE by considering a set of weakly coupled parallel wires. First, we will show that an infinite array of wires, where the first and second wires (in each unit cell) contain electrons in a positive orbital magnetic field, and the third and fourth wires contain holes in a negative field, can create a CI (see Fig. 1a). We then introduce a tight-binding version of this model and obtain a phase diagram, showing the Chern number as a function of the model parameters.

Kane et al. [6] generalized the wires approach to the Abelian fractional quantum Hall effect (FQHE) using the bosonization technique. We will show that our wires construction can be generalized to the interacting case as well.

The key point is to define composite particles. This transformation maps the electrons and holes at $1/3$ filling to composite particles at filling 1. This will lead to a systematic construction of Fractional Chern insulators (FCI). The possibility of a FCI has recently been discussed quite extensively in the literature [7]. Numerical investigations [8–13] of lattice models with nearly flat bands presented strong evidence for FCI states. More general approaches, connecting the properties of the known FQHE states and analogous FCI states, were found [14, 15]. Here we present an alternative analytic

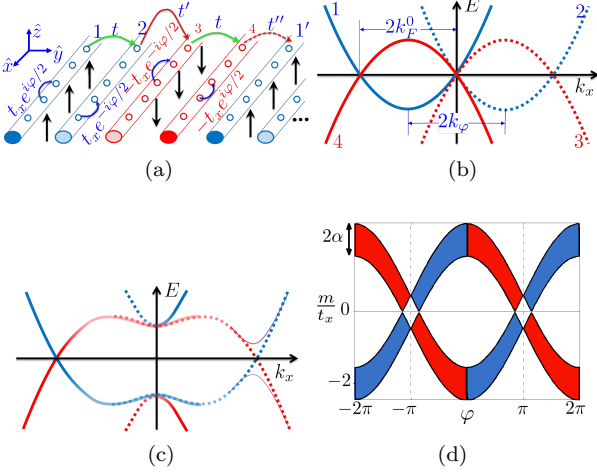


FIG. 1: (Color Online) (a) Physical scheme of the quasi-one-dimensional model we study. Blue wires contain electrons, and red wires contain holes. The black arrows represent the magnetic field through the system. The circles represent the sites of the corresponding tight binding model, and the tunneling amplitudes of the tight binding model are represented by colored arrows. (b) The energy spectrum of the wires (as a function of k_x) near zero energy without tunneling between the wires ($t, t', t'' = 0$). The mass term is chosen such that the four parabolas cross each other at zero energy. The spectra in blue, dashed blue, dashed red, and red correspond to wires 1, 2, 3, and 4 in a unit cell, respectively. k_F^0 is the Fermi k -vector in the absence of magnetic field and $k_F^0 a = \varphi/2$ is the shift of the spectra due to the magnetic field. (c) Thick lines show the energy spectrum when t is switched on. A gap opens near $k_x = 0$. The thin full lines show the spectrum when t' is switched on as well. This gives an additional gap at $k_x > 0$. Free chiral modes are left on wires 1 and 4. Notice that although the edge modes on wire 1 and 4 are at the same k -vector they remain gapless since the wires 1 and 4 are far apart in real space. Finally, if one switches on t'' , the tunneling between the unit cells, there are free chiral modes at the edge of the system. The presence of edge modes suggests that there is a non-zero Chern number, despite the zero average magnetic field. (d) The phase diagram showing the Chern number as a function of the mass m and the magnetic phase φ . Red regions have $C = 1$, blue regions have $C = -1$, and white regions are topologically trivial regions with $C = 0$. The figure was generated with the parameters $t/t_x = 0.5, t'/t_x = t''/t_x = 0.2$.

approach to the subject, which may be directly applicable to experiments.

Teo & Kane [16] expand the approach of [6] to non-Abelian states. We will see that our results can be generalized to the non-Abelian case as well, and we will provide a detailed construction of a state similar to the \mathbb{Z}_3 Read-Rezay state, which is particularly important, as it may be used for universal quantum computation. We expect this construction to be rather stable, as it is built from effective $\nu = 1/3$ states. Our construction will lack the disadvantages of one-dimensional systems, which are

sensitive to disorder [17, 18], and the need to invoke proximity to a superconductor and a strong magnetic field simultaneously [19–21].

Using an analogy between a magnetic field and a spin-orbit coupling (with an effective spin-orbit field in the \hat{z} direction only), we will construct a topological insulator from an array of wires. Here, instead of an alternating magnetic field, we will have alternating spin-orbit couplings. This way, all the states described above will have their time reversal invariant analogs.

Wires construction of a CI: Motivated by the above semi-classical picture, we have designed the wires construction, shown in Fig. 1a. In each unit cell there are four different wires. We tune the wires' chemical potentials such that wires 1 and 2 of each unit cell are near the bottom of the band, while wires 3 and 4 are near the top. Effectively, we have alternating pairs of wires that contain electrons and holes. A positive (negative) magnetic field is introduced between the pairs of electrons (holes) wires. This is a Q1D version of the semi-classical picture we described above.

For illustration and simplicity it is convenient to choose a gauge in which the vector potential \mathbf{A} points at the x direction. The spectra corresponding to different wires cross at several points. If we tune the wires' bands in such a way that all their crossing points match in energy, their energy spectra are similar to those found in Fig. 1b.

If in addition, neighboring wires of the same type are weakly tunnel coupled (with an amplitude t), a gap opens between parabolas 1 and 2, and parabolas 3 and 4. The spectrum in this case is depicted by the thick lines of Fig. 1c. The spectrum still has gapless modes: left mover on wire 1, right on 2, left on 3, and right mover on 4.

Introducing now a coupling between the electrons and holes *inside* a unit cell (t'), a gap will open at $k_x > 0$, and we arrive at the spectrum depicted by the thin lines of Fig. 1c. We still have nearly decoupled chiral states on wires 1 and 4. If we now switch on small tunneling between different unit cells (t''), the coupling between the edges decays exponentially with the sample width, and in the thermodynamic limit we expect to find gapless edge states. The observation of gapless edge states indicates that there is a non-zero Chern number.

Tight binding Model: To show this explicitly, we have constructed a 2-dimensional tight-binding model, which is the lattice version of the above continuous model (for more details see the supplemental material). The unit cell of the model is larger than the basic unit cell of the underlying square lattice - each unit cell contains 4 points, corresponding to the 4 different wires in Fig. 1a. Each point is characterized by (x, y) , the location of the unit cell (measured in units of the lattice spacing a), and $n = 1, 2, 3, 4$ which labels the sites inside the unit cell.

We introduce the nearest neighbor tunneling amplitudes: $t, t', t'', \pm t_x e^{\pm i k_F^0 a}$, described in Fig. 1a. The amplitude t_x describes tunneling along the wires, while $t, t',$

and t'' describe tunneling between different wires. The phase $e^{\pm i k_\varphi a}$, with $k_\varphi a = \frac{e B a^2}{2 \hbar c}$, is the Peierles phase associated with the alternating external magnetic field. It is related to the flux in a basic unit cell: $k_\varphi a = \frac{\varphi}{2}$, where $\varphi = 2\pi \frac{\Phi}{\Phi_0}$. In addition, we introduce a mass term (not related to the physical mass of the particle), which adds a constant energy m ($-m$) for electrons (holes). The sign of t_x is equal to the sign of the mass term. A change of the mass m shifts the spectra of the isolated wires up and down, and the magnetic flux shifts them left and right. Similar to Haldane's original model [4], m and φ tune the system into and out of the topological phases.

For simplicity, we restrict ourselves to the case $t'' = t'$. Using the particle-hole and inversion symmetries of the resulting Hamiltonian, we can find that the upper and lower bands cross each other when (see supplemental material)

$$\frac{m}{t_x} = \pm 2 \cos \frac{\varphi}{2} \pm \alpha, \quad (1)$$

with $\alpha = \sqrt{t^2 - t'^2}/t_x$ (in addition to the trivial crossings at $\varphi = 0, 2\pi$). These crossing points signal a topological phase transition between a trivial insulator and a Chern insulator. The full phase diagram, showing the Chern number as a function of φ and m , is depicted in Fig. 1d. We note that if we break the built in particle-hole symmetry of the model by adding a small chemical potential μ , metallic phases appear between the trivial and the Chern insulating phases. The boundaries of these metallic regions are $\frac{m}{t_x} = \pm 2 \cos \frac{\varphi}{2} \pm \alpha_\pm$, where $\alpha_\pm = \sqrt{(t \pm \mu)^2 - t'^2}/t_x$.

FCI: The wires construction invites us to add interactions and use bosonization techniques, similar to those used in [6, 16]. This allows us to generalize the above results to FCI states. In the presence of interactions, multi-electron processes may open a gap even if the Fermi point of the left movers is not equal to the Fermi points of the right movers [6, 16–18].

To understand the required conditions for a gap opening due to multi-electron scattering processes, it is useful to present the spectra of Fig 1b in an alternative way. Instead of plotting the entire spectrum of the wires together, we plot only the Fermi points as a function of the wire index. Soon, we will linearize the spectra around these points. A cross (\otimes) denotes the Fermi point of a left mover, and a dot (\odot) denotes the Fermi point of a right mover. Before analyzing the fractional case, it is useful to revisit the simple $\nu = 1$ case. We will see that the main results of the tight binding model arise naturally in the bosonization framework. Fig. 2a shows the diagram that corresponds this case (Fig. 1b). The Fermi point of the left mover of wire 1, for example, is $k_1^L = -k_F^0 - k_\varphi$. In the case $\nu = 1$, we have $k_F^0 = k_\varphi$, so that in units of k_φ we find $k_1^L = -2$. In the same way, one can find all the Fermi points shown in Fig. 2a.

Linearizing the spectrum around the Fermi-points of each

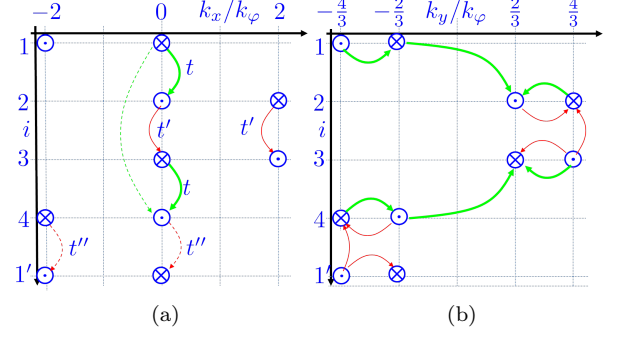


FIG. 2: (Color Online) (a) A diagrammatic representation of the energy band structure in the $\nu = 1$ case. The y axis shows the wire number inside the unit cell, and the x axis shows k_x in units of k_φ . The symbol \odot represents k_i^L and \otimes represents k_i^R of wire i . Colored arrows represent tunneling amplitudes between the wires. (b) The same diagram for a topological insulator with $\nu = \frac{1}{3}$. Colored arrows now represent the multi-electron processes responsible for the creation of Laughlin-like states. These complex processes in terms of the electrons ($\psi \sim e^{i\phi}$), can be regarded as simple tunneling processes in terms of the fermions $\tilde{\psi} \sim e^{i\eta}$. In the presence of spin orbit coupling, spin up (blue) and spin down (light red) will experience opposite alternating effective magnetic fields.

wire, and using the standard bosonization procedure, we define the two chiral bosonic fields, ϕ_i^R and ϕ_i^L , for each wire. In terms of these, the fermionic operators are

$$\psi_i^R \propto e^{i(k_i^R x + \phi_i^R)}, \quad \psi_i^L \propto e^{i(k_i^L x + \phi_i^L)}. \quad (2)$$

Without interactions, a momentum conserving single-electron tunneling between the wires (denoted in Fig. 2a by an arrow) is possible only when the left and right movers of adjacent wires are at the same point in k -space. The single-electron tunneling operators between adjacent wires (denoted in the figure by green, red, and dashed red arrows) are

$$\begin{aligned} t \psi_{1(3)}^{R\dagger} \psi_{2(4)}^L + h.c. &\propto t \cos(\phi_{1(3)}^R - \phi_{2(4)}^L) \\ t' \psi_2^{R(L)\dagger} \psi_3^{L(R)} + h.c. &\propto t' \cos(\phi_2^{R(L)} - \phi_3^{L(R)}) \\ t'' \psi_4^{R(L)\dagger} \psi_{1'}^{L(R)} + h.c. &\propto t'' \cos(\phi_4^{R(L)} - \phi_{1'}^{L(R)}). \end{aligned} \quad (3)$$

We switch on the operators in the following way: first, we switch on a small $t \ll t_x$. Since this is a relevant operator, it gaps out the spectrum near $k_x = 0$. Then, we switch on smaller electron-hole couplings $t', t'' < t$. The terms $\psi_2^{R\dagger} \psi_3^L$ and $\psi_4^{R\dagger} \psi_{1'}^L$ gap out the rest of the spectrum, leaving a gapless edge mode. As we discussed before, this indicates that there is a non-zero Chern number. Note that the terms $\psi_2^{L\dagger} \psi_3^R$ and $\psi_4^{L\dagger} \psi_{1'}^R$ contain fields which are conjugate to those already fixed by t . Strong

quantum fluctuations are therefore expected to suppress these terms.

We now turn to generalize this to Laughlin-like FCI states, with a filling factor $\nu = k_F^0/k_\varphi = 1/(2n+1)$, where n is a non-negative integer. For example, the k -vector pattern of the wires with $\nu = 1/3$ is shown in blue in Fig. 2b. In this case, multi-electron processes are expected to gap out the system (except for the edges). To see this, it is enlightening to define new chiral fermion operators

$$\begin{aligned}\tilde{\psi}_i^R &= (\psi_i^R)^{(n+1)}(\psi_i^{\dagger L})^n \propto e^{i(q_i^R x + \eta_i^R)}, \\ \tilde{\psi}_i^L &= (\psi_i^L)^{(n+1)}(\psi_i^{\dagger R})^n \propto e^{i(q_i^L x + \eta_i^L)},\end{aligned}\quad (4)$$

with

$$\begin{aligned}\eta_i^R &= (n+1)\phi_i^R - n\phi_i^L, \eta_i^L = (n+1)\phi_i^L - n\phi_i^R, \\ q_i^R &= (n+1)k_i^R - nk_i^L, q_i^L = (n+1)k_i^L - nk_i^R.\end{aligned}\quad (5)$$

A direct calculation of the commutation relations of the η -fields show that they have an additional factor of $2n\pi$ compared the ϕ -fields. This gives an extra (trivial) phase factor $e^{i2\pi n}$ in the anti-commutation relation of the $\tilde{\psi}$'s compared to the ψ 's, insuring that the $\tilde{\psi}$'s are fermionic operators. In addition, it can easily be checked that the resulting structure of the q 's is identical to that of the k 's in the case of $\nu = 1$ (Fig. 2a), so that $\tilde{\psi}$ can be regarded as a fermionic field at filling $\nu = 1$. This procedure can therefore be interpreted as an attachment of $2n$ quantum fluxes to each electron (similar to Jain's construction of composite fermions [22]).

Repeating the analysis of the $\nu = 1$ case, we can now write single $\tilde{\psi}$ tunneling operators, identical to those found in Eq. (3) (replacing $\psi \rightarrow \tilde{\psi}, \phi \rightarrow \eta$, with new tunneling amplitudes \tilde{t}, \tilde{t}' , and \tilde{t}''). In terms of the original electrons, these operators describe the multi-electron processes shown in Fig. 2b. Note that when the interactions are strong enough, these operators become relevant. From here, the process is identical to the integer case: first, we switch on \tilde{t} -terms and partially gap the spectrum. Then, we switch on smaller \tilde{t}', \tilde{t}'' -terms and gap out the entire spectrum, leaving chiral edge states. The gap due to the previous stage insures that competing processes (for example, single electron tunneling between wires 2 and 3, or 4 and 1') are suppressed because they contain fields that are conjugate to the fields pinned by \tilde{t} (which is dominant by our construction). The fact that the composite η -fields (and not the original ϕ fields) are pinned, leads to the various properties of these Laughlin-like states, like the fractional charge and statistics of the excitations, in analogy to the known FQHE states [6, 16].

Non-Abelian FCI: As the discussion above shows, the wires construction allowed us to create a variety of Abelian fractional Chern insulators. Ref. [16] constructed non-Abelian QHE states by enlarging the unit cell and taking a non uniform magnetic field inside each

unit cell. By our construction, any non-Abelian state constructed by [16] can be generalized to the CI case. To do so, one can take two unit cells from the construction in Ref. [16], reverse the magnetic field of the second unit cell, and take it to contain holes. However, the lack of total magnetic flux in our system allows for a simpler construction of non-Abelian states, which don't have a direct analog in the QHE. We now show that a slight modification of the procedure that enabled the construction of Laughlin-like states may lead to non-Abelian states. We will focus here on a state similar to the \mathbb{Z}_3 Read-Rezay state. Generalization to other non-Abelian states is possible.

To obtain the \mathbb{Z}_3 parafermion state we take $\nu = 1/3$, and construct the $\tilde{\psi}$ operators using Eq. (4). We switch on first the \tilde{t}' term leaving free left and right propagating $\tilde{\psi}$ on wires 1 and 4. If we now turn on smaller \tilde{t} , we generate (in a second order perturbation theory) an effective coupling of order \tilde{t}^2/\tilde{t}' between $\tilde{\psi}_1^R$ and $\tilde{\psi}_4^L$ (See dashed green line in Fig. 2a). If we approach the limit $\tilde{t}' \sim \tilde{t}$, we find that $\tilde{t}^2/\tilde{t}' \sim \tilde{t}$, so that the four operators $\tilde{\psi}_1^{\dagger R}\tilde{\psi}_4^L, \tilde{\psi}_1^{\dagger R}\tilde{\psi}_2^L, \tilde{\psi}_3^{\dagger R}\tilde{\psi}_2^L$ and $\tilde{\psi}_3^{\dagger R}\tilde{\psi}_4^L$ have similar amplitudes. Let us assume that we tune \tilde{t}, \tilde{t}' , and the coupling between $\tilde{\psi}_1^R$ and $\tilde{\psi}_4^L$, to have exactly the same value, denoted by v (at the end, when the topological nature of our construction will be revealed, this strict requirement can be relaxed, as long as the bulk gap never closes). In terms of the bosonized η fields, the resulting scattering term is: $v [\cos(\eta_2^L - \eta_1^R) + \cos(\eta_3^R - \eta_4^L) + \{2 \leftrightarrow 4\}]$. Defining $(\phi_c, \theta_c, \phi_s, \theta_s)^T = U(\eta_4^L, \eta_1^R, \eta_2^L, \eta_3^R)^T$, with $U = \frac{1}{\sqrt{24\pi}}(\sigma_x + \sigma_z) \otimes (\sigma_x + \sigma_z)$ (where σ_i are the pauli matrices), we find the Hamiltonian

$$\begin{aligned}\int \left[\frac{1}{2} \sum_{a=c,s} \left((\partial_x \phi_a)^2 + (\partial_x \theta_a)^2 \right) + 2 \cos(\sqrt{6\pi}\theta_c) \times \right. \\ \left. v \left[\cos(\sqrt{6\pi}\theta_s) + \cos(\sqrt{6\pi}\phi_s) \right] \right] dx dt.\end{aligned}\quad (6)$$

The term $\cos(\sqrt{6\pi}\theta_c)$ is relevant, and θ_c is therefore frozen at its minimum. Our problem is therefore mapped to the $\beta^2 = 6\pi$ self-dual Sine-Gordon model, which was studied in Ref. [23]. Specifically, it was shown that this model is mapped to a critical \mathbb{Z}_3 parafermionic field.

We have established that any unit cell has two counter propagating \mathbb{Z}_3 parafermionic fields (around $k = 0$), and two counter propagating charge modes at $k_x = -2k_\varphi$. As earlier, we can gap out the spectrum by turning on the \tilde{t}'' term between the unit cells, leaving eventually a Laughlin-like charge mode and a \mathbb{Z}_3 parafermion mode at the edge of the sample. We note that while the non-Abelian part is the same as the non-Abelian part of the \mathbb{Z}_3 Read-Rezay state, the charge mode is different.

Topological insulators from the wires approach: The entire analysis presented here can also be carried out for spinful electrons if one introduces spin-orbit interactions

(in the \hat{z} direction only). This can be done if an alternating electric field is introduced instead of an alternating magnetic field. The electric field should be tuned in such a way that the spin-orbit coupling is positive at wires 1 and 4, and negative at wires 2 and 3. For example, we depict in Fig. 2b the appropriate Fermi-momenta corresponding to $\nu = \frac{1}{3}$ (in blue for spin up and light red for spin down). If the tunneling between the wires conserves the spin, we get a simple construction for integer, Laughlin-like, and non-Abelian topological insulators [24]. We note that other processes, which may not conserve spin are possible. This can give rise to additional topological states.

Generalization: The approach we present here can be extended to hierarchical Abelian states, as well as other non-Abelian states (such as a Moore-Read-like state). One can also study the effects of proximity to a superconductor, which is expected to yield many other non-Abelian states. A detailed further study of these constructions will be performed in the future.

Experimental realizations: While the above construction is interesting from a purely theoretical standpoint, it may also be applicable to experiments. In practice, it should be possible to connect a few wires in a superlattice structure that will realize the particle-hole pattern we suggest. A superlattice of p-n junctions with a snake-like wire (see supplemental material) above it [25], creating an alternating magnetic field, may form a CI. Superlattices of materials with large spin-orbit coupling, such as InAs or InSb wires, may create a synthetic fractional topological insulator. Finally, stripes of alternating magnetic field can artificially be created in cold-atom systems [26].

Much work has been devoted in recent years into making a realistic system that supports non-Abelian states which allow universal quantum computation. Some works [17, 18] concentrated on one-dimensional systems, which are particularly sensitive to disorder [27, 28]. Other works [19, 21] utilized the stability of the FQHE states (which require a strong magnetic field) against disorder, and were able to show that they may support non-Abelian parafermion states when they are in proximity to a superconductor (which tends to repel magnetic fields, making these proposals experimentally challenging). Ref. [20] suggested a similar construction using a FCI.

Coupling many (or maybe only a few) wires together will reduce the effects of disorder. As long as the localization length of the edge modes is smaller than the sample width, it behaves practically as a two dimensional state. In addition, the spin-orbit coupling states we constructed don't require strong magnetic fields, which makes proximity to a superconductor possible.

Acknowledgments We would like to thank Arbel Haim, Erez Berg, Eran Sela, Ady Stern, Netanel Lindner,

Anna Kesselman for useful discussions. The work was supported by WIS-TAMU, ISF, Minerva and ERC (FP7/2007-2013) 340210 grants.

-
- [1] K. Klitzing, G. Dorda, and M. Pepper, *Physical Review Letters* **45**, 494 (1980).
 - [2] B. Halperin, *Physical Review B* **25**, 2185 (1982).
 - [3] D. Thouless, M. Kohmoto, M. Nightingale, and M. den Nijs, *Physical Review Letters* **49**, 405 (1982).
 - [4] F. D. M. Haldane, *Physical Review Letters* **61**, 2015 (1988).
 - [5] S. Sondhi and K. Yang, *Physical Review B* **63**, 054430 (2001).
 - [6] C. Kane, R. Mukhopadhyay, and T. Lubensky, *Physical Review Letters* **88**, 036401 (2002).
 - [7] S. A. Parameswaran, R. Roy, and S. L. Sondhi, *Comptes Rendus Physique* **14**, 816 (2013).
 - [8] E. Tang, J.-W. Mei, and X.-G. Wen, *Physical Review Letters* **106**, 236802 (2011).
 - [9] K. Sun, Z. Gu, H. Katsura, and S. Das Sarma, *Physical Review Letters* **106**, 236803 (2011).
 - [10] T. Neupert, L. Santos, C. Chamon, and C. Mudry, *Physical Review Letters* **106**, 236804 (2011).
 - [11] D. N. Sheng, Z.-C. Gu, K. Sun, and L. Sheng, *Nature communications* **2**, 389 (2011).
 - [12] Y.-F. Wang, H. Yao, Z.-C. Gu, C.-D. Gong, and D. N. Sheng, *Physical Review Letters* **108**, 126805 (2012).
 - [13] N. Regnault and B. A. Bernevig, *Physical Review X* **1**, 021014 (2011).
 - [14] X.-L. Qi, *Physical Review Letters* **107**, 126803 (2011).
 - [15] S. A. Parameswaran, R. Roy, and S. L. Sondhi, *Physical Review B* **85**, 241308 (2012).
 - [16] J. C. Y. Teo and C. L. Kane, (2011), [arXiv:1111.2617](#).
 - [17] Y. Oreg, E. Sela, and A. Stern, (2013), [arXiv:1301.7335](#).
 - [18] J. Klinovaja and D. Loss, (2013), [arXiv:1311.3259](#).
 - [19] N. H. Lindner, E. Berg, G. Refael, and A. Stern, *Physical Review X* **2**, 041002 (2012).
 - [20] A. Vaezi, (2013), [arXiv:1307.8069](#).
 - [21] R. S. K. Mong, D. J. Clarke, J. Alicea, N. H. Lindner, P. Fendley, C. Nayak, Y. Oreg, A. Stern, E. Berg, K. Shtengel, and M. P. A. Fisher, (2013), [arXiv:1307.4403](#).
 - [22] J. K. Jain, *Composite Fermions* (Cambridge University Press, 2007) p. 560.
 - [23] P. Lecheminant, A. O. Gogolin, and A. A. Nersisyan, *Nuclear Physics B* **639**, 502 (2002).
 - [24] M. Levin and A. Stern, *Physical Review Letters* **103**, 196803 (2009).
 - [25] G. Zeltzer (private communication).
 - [26] M. Aidelsburger, M. Atala, S. Nascimbène, S. Trotzky, Y.-A. Chen, and I. Bloch, *Physical Review Letters* **107**, 255301 (2011).
 - [27] L. Fidkowski and A. Kitaev, *Physical Review B* **83**, 075103 (2011).
 - [28] A. M. Turner, F. Pollmann, and E. Berg, *Physical Review B* **83**, 075102 (2011).

Supplemental Material

The supplemental material contains more details about the tight binding model introduced in the main text. A detailed derivation of the $m - \varphi$ phase diagram of Fig 1d is presented. In addition, we provide technical details about the experimental realization suggested at the concluding part of the main text.

Tight binding model

We define the annihilation operator, $c_n(x, y)$, for an electron in the wire n (with $(n = 1, 2, 3, 4)$) of the unit cell at position (x, y) .

The tight binding Hamiltonian, described in the main text, is a sum of the following terms:

$$H_m = m \sum_{x,y} \left[\sum_{n=1}^2 c_n^\dagger(x, y) c_n(x, y) - \sum_{n=3}^4 c_n^\dagger(x, y) c_n(x, y) \right], \quad (7)$$

$$H_y = -t \sum_{x,y} \left[c_2^\dagger(x, y) c_1(x, y) + c_4^\dagger(x, y) c_3(x, y) + h.c. \right], \quad (8)$$

$$H'_y = -t' \sum_{x,y} \left[c_3^\dagger(x, y) c_2(x, y) + c_1^\dagger(x, y+4) c_4(x, y) + h.c. \right], \quad (9)$$

$$H_x = -t_x \sum_{x,y} \left[c_n^\dagger(x+1, y) c_n(x, y) e^{i\phi_n} - c_n^\dagger(x+1, y) c_n(x, y) e^{i\phi_a} + h.c. \right], \quad (10)$$

with $\phi_1 = \phi_4 = -k_\varphi a = \varphi/2$ and $\phi_2 = \phi_3 = k_\varphi a = -\varphi/2$.

It is convenient to move to Fourier space, where the Hamiltonian takes the form $H = \sum_{\mathbf{k} \in BZ1} \psi^\dagger(\mathbf{k}) h(\mathbf{k}) \psi(\mathbf{k})$, with $\psi = (c_1, c_2, c_3, c_4)^T$, and

$$h(\mathbf{k}) = \begin{pmatrix} m - 2t_x \cos[(k_x - k_\varphi) a] & -t & 0 & -t' e^{4ik_y a} \\ -t & m - 2t_x \cos[(k_x + k_\varphi) a] & -t' & 0 \\ 0 & -t' & -m + 2t_x \cos[(k_x + k_\varphi) a] & -t \\ -t' e^{-4ik_y a} & 0 & -t & -m + 2t_x \cos[(k_x - k_\varphi) a] \end{pmatrix}. \quad (11)$$

We define a new gauge:

$$\begin{aligned} c_1(\mathbf{k}) &\rightarrow c_1(\mathbf{k}) e^{-ik_y a}, c_2(\mathbf{k}) \rightarrow c_2(\mathbf{k}) e^{-ik_y a}, \\ c_3(\mathbf{k}) &\rightarrow c_3(\mathbf{k}) e^{ik_y a}, c_4(\mathbf{k}) \rightarrow c_4(\mathbf{k}) e^{ik_y a}, \end{aligned} \quad (12)$$

in terms of which the Hamiltonian takes the simple form

$$\begin{aligned} h(\mathbf{k}) &= [m - 2t_x \cos(k_x a) \cos(k_\varphi a)] \sigma_z - 2t_x \tau_z \sin(k_x a) \sin(k_\varphi a) \\ &\quad - t \tau_x - t' \sigma_x [\cos(2k_y a) \tau_x - \sin(2k_y a) \tau_y], \end{aligned} \quad (13)$$

where τ_i ($i = x, y, z$) in Eq. (13) are Pauli matrices which operate within the 2×2 blocks separately, while σ_i are Pauli matrices which operate on the outer 2×2 matrix of blocks.

Symmetries

It is easy to check that the Hamiltonian in Eq. (13) has a particle-hole symmetry,

$$\Lambda h(\mathbf{k}) \Lambda = -h^*(-\mathbf{k}), \quad (14)$$

where $\Lambda = \sigma_x \tau_z$. The particle-hole symmetry implies that the bands are symmetric around $E = 0$. Therefore, any crossing of the upper and lower bands must be at $E = 0$. Additionally, we have an inversion symmetry,

$$Ph(\mathbf{k})P = h(-\mathbf{k}), \quad (15)$$

where $P = \tau_x$. The crossings therefore must either be at the high symmetry points, satisfying $-\mathbf{k} = \mathbf{k} + \mathbf{G}$, or come in pairs.

Crossing points

For convenience, we write the Bloch Hamiltonian, Eq. (13), in the form

$$h = A\sigma_z + B\tau_z + C\tau_x + D\sigma_x\tau_x + E\sigma_x\tau_y. \quad (16)$$

In terms of these, the spectrum is

$$E = \pm \sqrt{(A^2 + B^2 + C^2 + D^2 + E^2)} \pm 2\sqrt{A^2B^2 + A^2C^2 + C^2D^2}. \quad (17)$$

Using this explicit form, it is now easy to find that the upper and lower bands cross each other at the high symmetry points when

$$m = \pm 2t_x \cos(k_\varphi a) \pm \sqrt{t^2 - t'^2}. \quad (18)$$

These crossing points signal a topological phase transition between a topologically trivial phase and a phase with a non-zero chern number.

There are additional crossings at the points $k_\varphi a = 0, \pi$, whose locations depend on m . Since these crossings are not at the high symmetry points, they must come in pairs.

If we add a small, non-zero, chemical potential μ , the bands cross the chemical potential when

$$m = \pm 2t_x \cos(k_\varphi a) \pm \sqrt{(t \pm \mu)^2 - t'^2}. \quad (19)$$

The topologically trivial and non-trivial insulating phases are now separated by metallic phases. The transitions between the metallic and insulating phases are described by Eq. (19).

In the same way, metallic regions appear near $k_\varphi a = 0, \pi$.

Experimental realization

Our Q1D construction requires an alternating magnetic field. Experimentally, this can be realized using a snake-like wire, similar the one shown in Fig. 3.

In this configuration, we get that the desired current, needed to create the states we constructed, is of order

$$I \sim \frac{n\pi\hbar c^2}{2e} \approx 100mA \frac{n}{(100nm)^{-1}},$$

where n is the one-dimensional density of the conducting band. Assuming $n^{-1} \sim 100nm$, we get that currents of order $\sim 100mA$, should suffice.

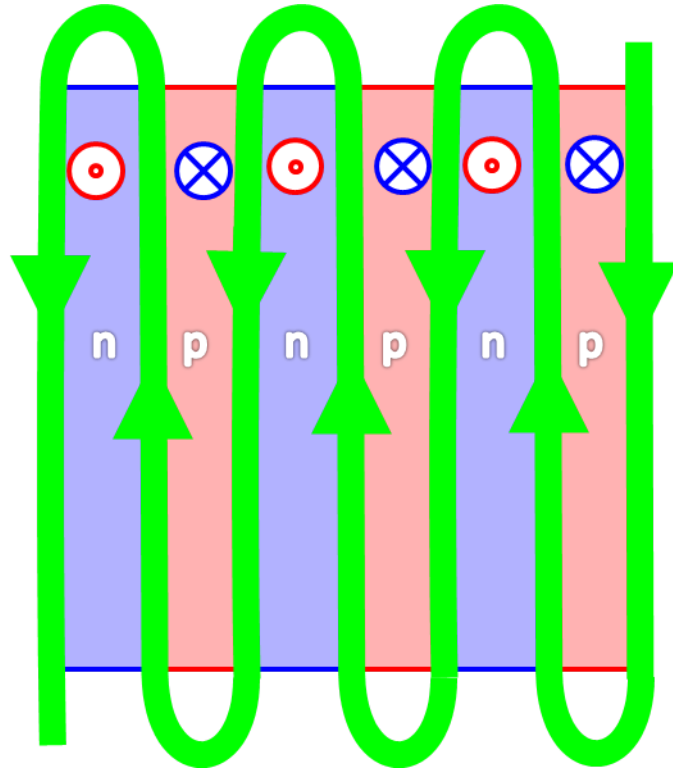


FIG. 3: A possible experimental realization of our construction. Green lines represent current carrying wires, which produce the alternating magnetic field needed for our construction. This way, the magnetic field is positive (i.e. out of the page, denoted by \odot) in n -regions that contain electrons, and negative (\otimes) in p -regions that contain holes.